

Shear-Layer Instabilities of a Pulsed Stack-Issued Transverse Jet

Ching M. Hsu, Rong F. Huang, and Michael E. Loretero

Abstract—Shear-layer instabilities of a pulsed stack-issued transverse jet were studied experimentally in a wind tunnel. Jet pulsations were induced by means of acoustic excitation. Streak pictures of the smoke-flow patterns illuminated by the laser-light sheet in the median plane were recorded with a high-speed digital camera. Instantaneous velocities of the shear-layer instabilities in the flow were digitized by a hot-wire anemometer. By analyzing the streak pictures of the smoke-flow visualization, three characteristic flow modes, *synchronized flapping jet*, *transition*, and *synchronized shear-layer vortices*, are identified in the shear layer of the pulsed stack-issued transverse jet at various excitation Strouhal numbers. The shear-layer instabilities of the pulsed stack-issued transverse jet are synchronized by acoustic excitation except for transition mode. In transition flow mode, the shear-layer vortices would exhibit a frequency that would be twice as great as the acoustic excitation frequency.

Keywords—Acoustic excitation, jet in crossflow, shear-layer instability.

I. INTRODUCTION

A jet deflected in a crossflow, which is a “transverse jet,” has been studied for many years, and is important in various practical engineering applications such as combustion, industrial mixing, injection cooling, and pollution transport. The subject is commonly identified in two categories according to the jet’s source—the jet may eject from an orifice on a wall [1]-[3] or from an elevated stack (or tube) [4]-[6]. The wall-issued transverse jet is often encountered in the film cooling of jet engines, power-plant combustors, V/STOL airplanes, turbine-blade cooling, and so on. The presence of stack-issued transverse jet characterizes many situations of technological importance in the environmental field, e.g., the stack flares and plume dispersion. The wall-issued transverse jet is characterized by three-dimensional flows, which are subject to interactions among the jet, jet-wake, and wall-boundary layer whereas the flow structures in the stack-issued transverse jet are subject to the interactions among the jet, jet-wake, and stack-wake. The common feature of the time-averaged flow structure of the wall-issued and stack-issued transverse jets is

the counter-rotating vortex pair associated with the jet cross-section appearing in the far field.

The mixing process of the wall-issued transverse jet can be improved by pulsating the jet flow. Several methods, such as the acoustic excitation, piezoelectric actuator and solenoid valve, have been applied to generate jet velocity oscillation. Recent investigations [7]-[12] revealed that jet velocity oscillation increased jet penetration and spread when a transverse jet is subjected to the specific excitation conditions of acoustic waves. Gogineni et al. [7] utilized the piezoelectric actuators mounted on the interior walls of a square jet to modulate an air jet in crossflow. They found that manipulating the upstream and downstream segments of the jet shear layer increased jet penetration and mixing. A solenoid valve operated by a square wave signal of variable frequency, injection time, and duty cycle was used to pulse the transverse jet in a water tunnel [8]-[10]. Johari et al. [8] demonstrated that penetration of a fully modulated jet in crossflow can be characterized by injection time and duty cycle. A Long injection time yielded a moderate increase in mixing of a fully pulsed jet. Eroglu and Breidenthal [9] observed that the pulsed jet consists of a sequence of vortex rings that penetrate deeply into the crossflow. A classification scheme proposed by [10] demarcated the various flow regimes of a pulsed jet depending on the stroke ratio and duty cycle. M’Closkey et al. [11] and Shapiro et al. [12], who acoustically excited a transverse air jet in a wind tunnel, demonstrated that in some cases, applying forcing frequencies corresponding to sub-harmonics of the upstream shear layer mode for the unforced transverse jet increased jet penetration. In other scenarios, merely exciting at the optimal pulse width and low excitation frequency yielded the best jet penetration and spread.

Although the pulsed wall-issued transverse jet at various pulsating configurations has been studied extensively, investigations of characteristic flow behaviors and shear-layer instabilities for the pulsed stack-issued transverse jet are rare. In this study, the flow visualization technique was applied to observe the characteristic flow behaviors of a pulsed stack-issued transverse jet. The hot-wire anemometer was used to detect the velocity profiles of the shear-layer instabilities of the pulsed stack-issued transverse jet. The aims of this study were to identify the characteristic of shear-layer instabilities of a stack-issued transverse jet subjected to excitation by acoustic wave.

C. M. Hsu is with the Graduate Institute of Applied Science and Technology, National Taiwan University of Science and Technology, Taipei 10607, Taiwan, ROC (phone: +886-2-2737-6940; fax: +886-2-2730-3733; e-mail: cmhsu@mail.ntust.edu.tw).

R. F. Huang is with the Department of Mechanical Engineering, National Taiwan University of Science and Technology, Taipei 10607, Taiwan, ROC (e-mail: rfhuang@mail.ntust.edu.tw).

M. E. Loretero is with the Department of Mechanical Engineering, University of San Carlos, Cebu, 6000, Philippines (e-mail: meloretero@usc.edu.ph).

II. EXPERIMENTAL METHODS

A. Experimental Set-up

The experimental apparatus and coordinate system are shown in Fig. 1. The experiments were conducted in an open-circuit type wind tunnel with a test section of $30 \times 30 \times 110$ cm. The wind tunnel is capable of crossflow velocities between 0.5 and 15 m/s with the turbulence intensity and non-uniformity under 0.25% and 0.4%, respectively. A stainless steel tube with an inner diameter $d = 5$ mm, an outer diameter $D = 6.4$ mm, and a length $L = 510$ mm was adapted to the tip of a nozzle assembly. This tube was perpendicularly protruded into the test section to serve as a stack. The protruding tube height measured from the test section floor to the end was 160 mm. The crossflow velocity (u_w) was measured by a Pitot static tube associated with a high-precision electronic pressure transducer. The average exit velocity of the jet (u_j) was monitored by a calibrated rotameter. The crossflow Reynolds numbers, Re_w , based on the outer diameter of the tube and the crossflow velocity, were fixed at 1710. The jet Reynolds number, Re_j , based on the inner diameter of the tube and average exit velocity of jet (u_j), was 1000. Consequently, the jet-to-crossflow momentum flux ratio defined by $R = \rho_j u_j^2 / \rho_w u_w^2$, where ρ_j and ρ_w are the jet and crossflow densities, respectively, was fixed at 0.56. The coordinate system is centered at the jet exit, with x in the axial direction, y in the lateral direction, and z in the transverse direction, as shown in the sub-figure of Fig. 1. Upstream of the nozzle assembly was a plenum on which was mounted a loudspeaker used for acoustic excitation of the jet. A square wave with a duty cycle of 50%, generated by a function generator and amplified by a power amplifier, was used to drive the loudspeaker. The excitation frequencies (f_{exc}) of the loudspeaker were varied from 60 Hz to 1000 Hz. The excitation voltage (E_{exc}) was fixed at 10V.

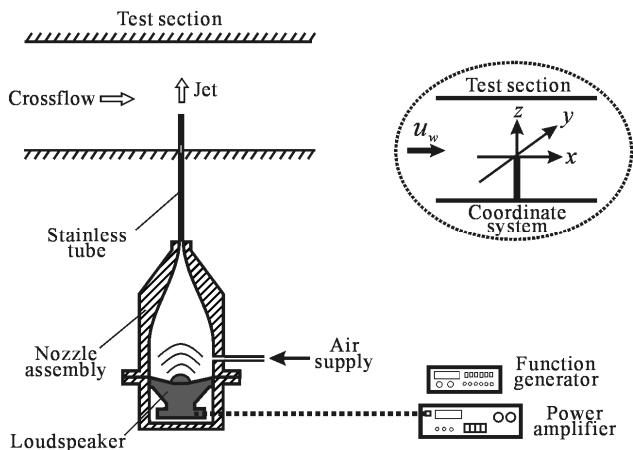


Fig. 1 Experimental setup

B. Flow Visualization

The instantaneous flow patterns were visualized by using the Mie scattering technique. To scatter the laser light, the kerosene oil-mist particles were seeded into the jet. The diameter and density of the kerosene oil-mist particles were $4.7 \pm 0.2 \mu\text{m}$ and

5.31 kg/m^3 , respectively. The Stokes number [13] was smaller than 1×10^{-3} , which is sufficiently small to ensure that the particles follow the flow. The light source for flow visualization was a high-repetition-rate, dual-head diode-pumped Nd:YLF (Neodymium Doped Lithium Yttrium Fluorides) laser. The wavelength of the light beams emitted from the laser head was 527 nm. By using a set of optics, the laser beam was bundled in a planar laser sheet with a thickness being about 0.5 mm. The laser sheet was aligned vertically from a transparent glass-window on the top of the wind-tunnel test section's ceiling so that the particles on the flowfield's symmetry plane would be illuminated during observation of the median plane's flow patterns. A high-speed camera (IDT X-stream XS-4) was used to capture the streak images of the laser-light sheet-illuminated smoke-traced flow patterns on the median plane $y = 0$.

C. Instability Frequency Detection

A one-component hot-wire anemometer was used to detect the traveling vortical instabilities in the upwind shear layer or in the oscillating motions of the deflected jet. In order to detect properly the frequency of the instability motions, the probe position underwent careful adjustment and, thereby, captured the oscillation signals caused by the swept-over character of the vortices or of the oscillation waves. To analyze the dynamic behaviors and to calculate the flow statistics, the current study fed the output signals of the hot-wire anemometer simultaneously into an FFT analyzer and a high-speed PC-based data-acquisition system. During the experiment, the FFT analyzer served to monitor the output signals of the hot-wire anemometer relative to the time and frequency domains, thereby ensuring the appropriateness of the probe position at all times. The hot-wire probe used was TSI 1210-T1.5, which could be applied in either end flow or the cross flow. The original tungsten wire was replaced by platinum wire. The wire diameter and length were $5 \mu\text{m}$ and 1.5 mm, respectively. The dynamic response corresponding to the electronic square-wave test was adjusted to 20 kHz. The sampling rate and the elapse time of the data-acquisition system were set to 23,000 samples/second and 7 seconds. The accuracy for the hot-wire probe positioning was 10 mm. The accuracy of the instability frequencies depended not only on the response of the hot-wire anemometer but also on the record length and the sampling rate of the FFT analyzer. The uncertainty of the frequency detection was estimated to be within ± 0.75 percent of the reading in this study.

III. RESULTS AND DISCUSSION

A. Jet Pulsation

As the crossflow was not applied, the one-component hot-wire anemometer was used to measure the jet-exit velocity pulsations at $(x/d, y/d, z/d) = (0, 0, 0.6)$. Fig. 2 shows variations of the detected jet-exit velocity u_{j0} with time at various excitation Strouhal numbers St_{exc} ($St_{exc} = f_{exc} d / u_j$, where f_{exc} denotes the frequency of acoustic excitation, d is the inner diameter of the tube, and u_j is the average velocity of the jet at the tube exit) with a jet Reynolds number of $Re_j = 1000$. The

jet-exit velocity wave forms of all excited jets behave periodical pulsation. At a St_{exc} smaller than about 0.5, the peak-to-peak values of the pulsatile wave forms were large. It was about 4.5m/s at $St_{exc} = 0.10$. At $St_{exc} = 0.45$ ($f_{exc} = 270$ Hz), the peak-to-peak value specifically attained about 12.5m/s. At a St_{exc} greater than about 0.5, the peak-to-peak values of the pulsatile wave forms dropped drastically. For example, the values were about 0.5m/s and 0.6m/s at $St_{exc} = 0.67$ ($f_{exc} = 400$ Hz) and $St_{exc} = 0.84$ ($f_{exc} = 500$ Hz), respectively, as shown in Figs. 2 (c) and (d). The frequency of the pulsatile wave form for each acoustic excitation condition is the same as the excitation frequency.

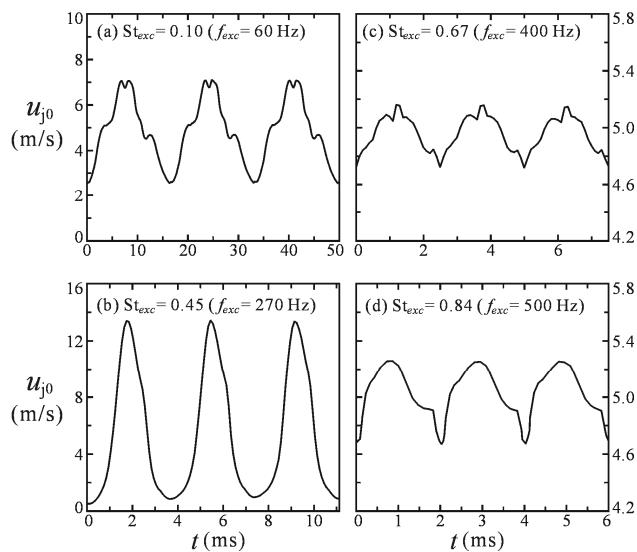


Fig. 2 Velocity histories of jet at tube exit. $Re_j = 1000$

B. Characteristic Flow Behavior

Fig. 3 shows typical instantaneous flow patterns in the median plane of the non-excited and excited stack-issued transverse jets at $R = 0.56$ obtained by the laser-assisted smoke-flow visualization technique. For non-excited case, as shown in Fig. 3 (a), a clear mushroom-shaped flow structure (indicated by an arrow) appears on the upwind side of the deflected jet after the jet leaves the tube-tip a distance of about $1d$. According to the observation of Huang and Lan [5], this type of flow structure is termed the “*swing-induced mushroom vortices*.” In general, this type of flow structure occurs in the range of $0.49 < R < 1.01$. At $St_{exc} = 0.10$ ($f_{exc} = 60$ Hz), as shown in Fig. 3 (b), the jet column evolved from the jet exit tilts up and down due to the jet-exit velocity pulsation. Therefore, a wavy flow structure is induced in the downstream area of the deflected jet. The periodically created wavy flow structure propagates downstream and causes the deflected jet to oscillate. This situation is quite similar to that of swing a rope by holding the rope at the jet exit. At $St_{exc} = 0.45$ ($f_{exc} = 270$ Hz), as shown in Fig. 3 (c), a puff flow structure (indicated by an arrow) is evolved from the jet exit within one excitation cycle because of the up-and-down jet column induced by the large jet velocity pulsation. This process continuous for each excitation cycle and

thus a series of puffs appears in the upper part of the deflected jet. The characteristic flow patterns in Figs. 3 (b) and (c) are induced by the periodic up-and-down oscillating motion of the jet column. Therefore, a pulsed stack-issued transverse jet behaves like the patterns shown in Figs. 3 (c) and (d) is termed the “*synchronized flapping jet*.” At $St_{exc} = 0.67$ ($f_{exc} = 400$ Hz), as shown in Fig. 3 (d), two backward-rolling vortices (indicated by arrow) evolve in the upwind shear layer of the deflected jet within one excitation. At $St_{exc} = 0.84$ ($f_{exc} = 500$ Hz) and $St_{exc} = 1.40$ ($f_{exc} = 830$ Hz), as shown in Figs. 3 (e) and (f), one mushroom-shaped vortex (indicated by arrow) evolves in the upwind shear layer of the deflected jet within one excitation cycle. Comparing the flow pattern of Fig. 3 (d) with that of Fig. 3 (e) indicates that the numbers of vortex evolving in the shear layer of the deflected jet are synchronized by acoustic excitation frequency for Fig. 3 (b). The flow characteristic behaves like the flow pattern shown in Fig. 3 (e) is termed the “*synchronized shear-layer vortices*” flow mode. While flow characteristic behaves like the flow pattern shown in Fig. 3 (d) is termed the “*transition*” flow mode.

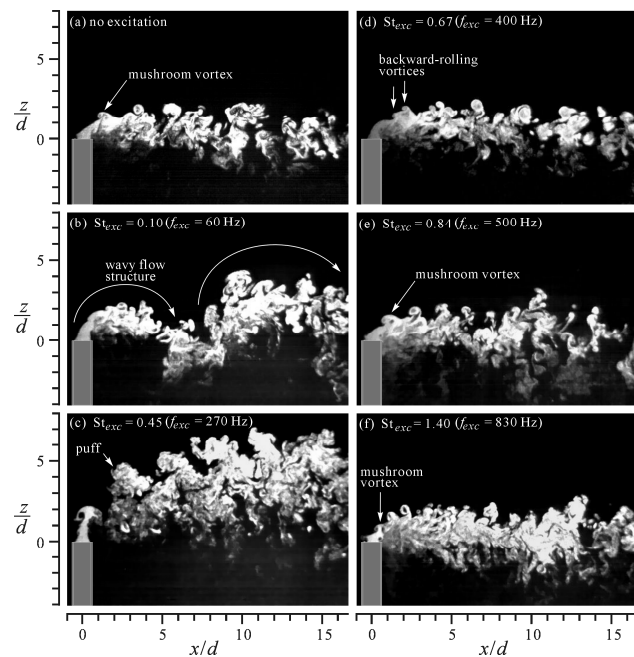


Fig. 3 Characteristic flow patterns in the median plane of the non-excited and excited transverse jet. $R = 0.56$, $Re_j = 1000$. Exposure time: $1/10,000$ s. (a) no excitation, (b) jet oscillation mode, (c) puff mode, (d) transition mode, (e), (f) synchronized shear-layer vortices mode

C. Shear Layer Instability

Placing a hot-wire anemometer probe at a position near the tube exit and fine tuning the probe location, we detected the velocity histories u of the jet-instability waves. The typical hot-wire signals and the corresponding power spectrum density function at various excitation Strouhal numbers are shown in Figs. 4 and 5. Figs. 4 (a) and (b) show the condition of the non-excited case. The hot-wire probe was placed at $(x/d, z/d) =$

(2, 2). The velocity histories, as shown in Fig. 4 (a), are periodic sinusoid-like wave forms. To obtain the characteristic frequency of the instability waves, we transformed the velocity histories in the time domain to power-spectrum density functions in the frequency domain by using the discrete fast Fourier transform (DFFT) technique. The natural frequency of the shear-layer instability identified in the power spectrum density function (as shown in Fig. 4 (b)) is 377 Hz. For the jet oscillation flow in synchronized flapping jet mode, the velocity histories were measured at $(x/d, z/d) = (2, 2)$, as shown in Fig. 4 (c). The periodic signals fluctuate drastically. The peak-to-peak values of the velocity signals are anomalously large (about 4 m/s) since the excitation pulsation velocity were relatively large, as is shown in Fig. 2 (a). The characteristic frequency identified by the peak frequency in Fig. 4 (d) is 60 Hz. This result reveals that the oscillating frequency of the deflected jet is synchronized by the acoustic excitation frequency. For the puff flow in the synchronized flapping jet mode, the velocity histories were measured at $(x/d, z/d) = (2, 4)$, as shown in Fig. 4 (e). The velocity signals behave periodic and irregular. The characteristic frequency identified by the peak frequency in Fig. 4 (f) is 270 Hz. Therefore, the frequency of the puffs evolving in the upwind shear layer of the deflected jet coincides with the acoustic excitation frequency.

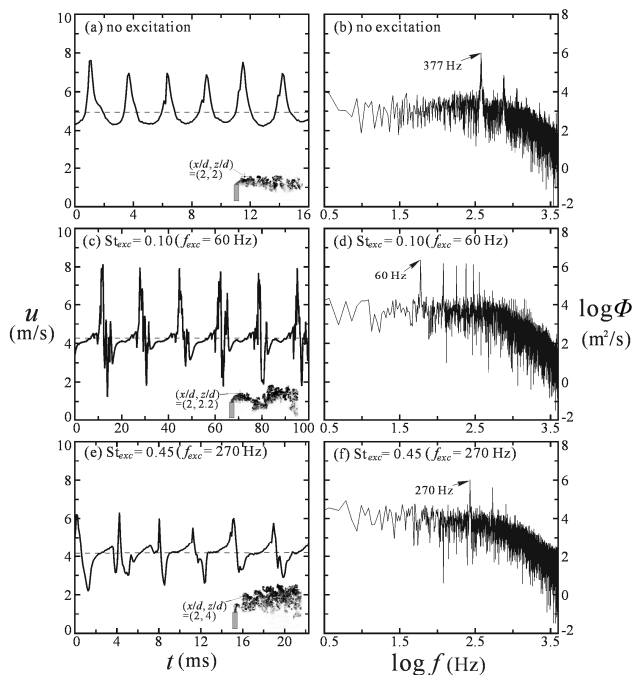


Fig. 4 Typical hot-wire signals (a), (c), (e) and the corresponding power spectral density function (b), (d), (f). $R = 0.56$, $Re_j = 1000$. (a), (b) no excitation, (c)-(f) synchronized flapping jet mode

In the transition flow mode, the velocity histories were measured at $(x/d, z/d) = (2, 2.2)$, as shown in Fig. 5 (a). The wave forms changed drastically when compared with that in Figs. 4 (c) and (e)—the magnitude of the pulsating waves decreased drastically and each periodic hump comprised dual

sub-humps (as indicated by the arrow heads). Because two vortices (which were somewhat close to each other) emerged in one period of acoustic excitation in the transition mode, as is shown in Fig. 3 (d), each sub-hump therefore signatures swept-over of one single shear-layer vortex. The peak frequency identified by the peak frequency in Fig. 5 (b) is 800 Hz. Fig. 5 (c) shows the condition of the synchronized shear-layer vortices flow mode. The velocity histories were measured at $(x/d, z/d) = (2, 2)$. The amplitudes of the signals are a little larger than those of Fig. 5 (a), and the wave forms present a single hump corresponding to each excitation period, which is consistent with the observed features of Fig. 3 (e). Therefore, the peak frequency identified in Fig. 5 (d) is the same as acoustic excitation. In Figs. 5 (e) and (f), the characteristic frequency and velocity signals of the shear-layer instability are similar to those of Figs. 5 (c) and (d). Results of the measured instability frequencies verify quantitatively the flow visualization results as described in the above paragraphs.

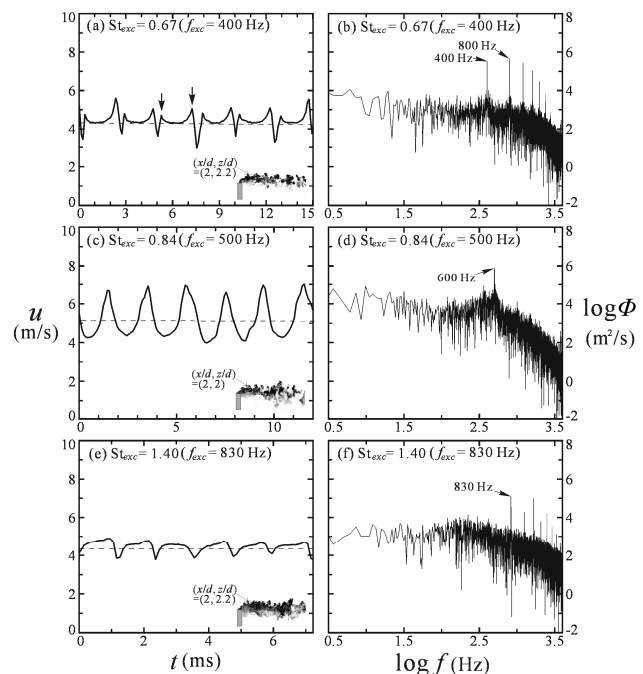


Fig. 5 Typical hot-wire signals (a), (c), (e) and the corresponding power spectral density function (b), (d), (f). $R = 0.56$, $Re_j = 1000$. (a), (b) transition mode, (c)-(f) synchronized shear-layer vortices mode

As discussed in the above paragraphs regarding $R = 0.56$, the characteristic flow behaviors of the jet instabilities varies with excitation Strouhal numbers. Three characteristic flow modes, *synchronized flapping jet*, *transition*, and *synchronized shear-layer vortices*, are identified in the shear layer of the pulsed stack-issued transverse jet at various excitation Strouhal numbers. We obtained the boundaries by examining the streak smoke-flow pictures. The boundaries separating the *synchronized flapping jet* and the *transition* regimes as well as the *transition* and *synchronized shear-layer vortices* regimes are about $St_{exc} = 0.53$ and $St_{exc} = 0.82$, respectively. The corresponding excitation frequencies are 330 Hz and 475 Hz,

respectively. In the synchronized flapping jet regime ($St_{exc} < 0.53$), the jet column near the tube exit swings back-and-forth and induces large up-down oscillating motions in the deflected jet (similar to Figs. 3 (b) and (c)). The oscillating-jet frequency coincides with the frequency of acoustic excitation. In the synchronized shear-layer vortices regime ($St_{exc} > 0.82$), a mushroom vortex evolves on the upwind shear layer of the deflected jet (similar to Figs. 3 (e) and (f)). The frequency of the upwind shear-layer instability is synchronized with the acoustic excitation frequency. In the transition regime (the excitation Strouhal number between about 0.53 and 0.82), a backward-rolling vortices appear on the upwind shear-layer of the deflected jet (similar to Fig. 3 (d)), but the frequency of the shear-layer instability is twice as great as the excitation frequency.

IV. CONCLUSIONS

The current study has experimentally examined the characteristic flow behavior and instantaneous velocities of the pulsed stack-issued transverse jet. We identified three characteristic flow modes—*synchronized flapping jet*, *transition*, and *synchronized shear-layer vortices* modes. The synchronized flapping jet appeared in the regime the excitation Strouhal numbers was lower than 0.53 ($f_{exc} < 310$ Hz). The synchronized shear-layer vortices were observed in the regime the excitation Strouhal numbers was larger than 0.82 ($f_{exc} > 480$ Hz). The transition regime existed in-between of the above two modes. When the jet was forced into the synchronized flapping jet regime, the jet column near the tube exit swung back-and-forth periodically at the excitation frequency and hence induced large up-down motions in the deflected jet. Forcing the jet in the transition and synchronized shear-layer vortices regimes caused the vortices to appear along the upwind shear layer of the deflected jet at a frequency twice of the excitation frequency and the excitation frequency, respectively.

REFERENCES

- [1] Y. Kamotani, and I. Greber, "Experiments on a turbulent jet in a crossflow," *AIAA Journal*, vol. 10, 1972, pp. 1425 - 1429.
- [2] T. F. Fric, and A. Roshko, "Vortical structure in the wake of a transverse jet," *Journal of Fluid Mechanics*, vol. 279, 1994, pp. 1-47.
- [3] R. M. Kelso, T. T. Lim, and A. E. Perry, "An experimental study of round jets in cross-flow," *Journal of Fluid Mechanics*, vol. 306, 1996, pp. 111-144.
- [4] O.S. Eiff, and J.F. Keffer, "On the structures in the near-wake region of an elevated turbulent jet in a crossflow," *Journal of Fluid Mechanics*, vol. 333, 1997, pp.161-195.
- [5] R.F. Huang, and J. Lan, "Characteristic modes and evolution processes of shear-layer vortices in an elevated transverse jet," *Physics of Fluids*, vol. 17, No. 3, 2005, pp. 1-13.
- [6] M. S. Adaramola, D. Sumner, and D. J. Bergstrom, "Turbulent wake and vortex shedding for stack partially immersed in a turbulent boundary layer," *Journal of Fluids and Structures*, vol. 23, 2007, pp. 1189-1206.
- [7] S. Gogineni, L. Goss, and M. Roquemore, "Manipulation of a jet in crossflow," *Experimental Thermal and Fluid Science*, vol. 16, 1998, pp. 209-219.
- [8] H. Johari, M. Pacheco-Tougas, J.C. Hermanson, "Penetration and mixing of fully modulated turbulent jets in crossflow," *AIAA Journal*, vol. 37, 1999, pp. 842-850.
- [9] A. Eroglu, R.E. Breidenthal, "Structure, penetration, and mixing of pulsed jets in crossflow," *AIAA Journal*, vol. 39, 2001, pp. 417-423.
- [10] H. Johari, "Scaling of fully pulsed jets in crossflow," *AIAA Journal*, vol. 44, 2006, pp. 2719-2725.
- [11] R.T. M'Closkey, J.M. King, L. Cortelezzi, A.R. Karagozian, "The actively controlled jet in crossflow," *Journal of Fluid Mechanics*, vol. 452, 2002, pp. 325-335.
- [12] S.R. Shapiro, J.M. King, R.T. M'Closkey, A.R. Karagozian, "Optimization of controlled jets in crossflow," *AIAA Journal*, vol. 44, 2006, pp. 1292-1298.
- [13] R. C. Flagan, and J. H. Seinfeld, *Fundamentals of Air Pollution Engineering*, Prentice Hall, Englewood Cliffs, New Jersey, 1988, pp. 290-357.